

# Three dimensional MEMS microfluidic perfusion system for thick brain slice cultures

Yoonsu Choi · Maxine A. McClain ·  
Michelle C. LaPlaca · A. Bruno Frazier · Mark G. Allen

Published online: 8 November 2006  
© Springer Science + Business Media, LLC 2007

**Abstract** *In vitro* tissue culture models are often benchmarked by their ability to replicate *in vivo* function. One of the limitations of *in vitro* systems is the difficulty in preserving an orchestrated cell population, especially for generating three-dimensional tissue equivalents. For example, tissue-engineering applications involve large high-density constructs, requiring a perfusing system that is able to apply adequate oxygen and nutrients to the interior region of the tissue. This is particularly true with respect to thick tissue sections harvested for *in vitro* culture. We have fabricated a microneedle-based perfusion device for high-cell-density *in vitro* tissue culture from SU-8 photosensitive epoxy and suitable post-processing. The device was tested for its ability to improve viability in slices of harvested brain tissue. This model was chosen due to its acute sensitivity to disruptions in its nutrient supply. Improved viability was visible in the short term as assessed via live-dead discriminating fluorescent staining and confocal microscopy. This perfusion system opens up many possibilities for both neurobiological as well as other culture systems.

**Keywords** Microneedle · SU-8 · Hippocampal brain slices

---

Y. Choi · M. A. McClain (✉) · A. B. Frazier · M. G. Allen  
School of Electrical and Computer Engineering, Georgia Institute of Technology,  
791 Atlantic Dr. Atlanta, 30332-0250 GA  
e-mail: Maxine.mcclain@gatech.edu

M. C. LaPlaca  
Department of Biomedical Engineering, Georgia Institute of Technology,  
513 First Dr. Atlanta, 30332-0250 GA

## Introduction

Dense multi-layer cell culture has been important in tissue engineering because replication of certain *in vivo* functions requires minimum cell-cell interaction functioning in a synchronous manner (Vunjak-Novakovic et al., 2006; Wu et al., 2005). *In vitro* microscale tissue perfusion has been used to study functional parameters (i.e. tissue equivalents)(Gomes et al., 2006a; Mehta and Linderman 2006; Xu et al., 2006), and to generate tissue intended for *in vivo* use (Bettinger et al., 2006; Gomes et al., 2006b). Brain tissue preparations are used extensively in neuroscience research because they possess organized networks that cannot be recreated in culture from individual cells, while the *in vivo* limitations of accessibility, immunological and inflammatory factors are avoided. They have been implemented extensively in basic electrophysiology to map network function in the brain (Wu et al., 2005; Wu et al., 2002). Brain tissue preparations have also been important in the areas of pharmacology and injury response (Gahwiler et al., 1997; Kristensen et al., 2003; Noraberg et al., 2000). Larger preparations that preserve more interconnections than thin slices, contain additional characteristic signals, making their successful preservation desirable for more extensive studies (Wu et al., 2005; Wu et al., 2002).

The time period of study for brain slice preparation ranges from several hours for acute slices to weeks or months for organotypic slices (Buckby et al., 2004; De Simoni et al., 2003). The limiting factor in maintaining healthy brain tissue *in vitro* is mass transport due to the lack of a circulatory system. Therefore, it is desirable to obtain a slice large enough to include networks of interest while still enabling adequate oxygen, nutrient and waste exchange in the interior of the tissue. If a mechanism could be put in place to address

the tissue's metabolic needs, the fidelity of the electrophysiology is expected to improve; consequently, the results of *in vitro* studies would more closely resemble their *in vivo* counterparts.

A three-dimensional (3-D) perfusion design can provide convective mass transport to the interior of the tissue for experiments on large tissue preparations over extended time periods. The fluidic channels are necessary for brain slice culturing since the capillaries in the slice do not function as flow vessels and therefore nutrients applied exogenously do not reach the interior cells in adequate quantities (Wu et al., 2005). Microneedle arrays offer the ability to replace this functionality; furthermore, they may be designed to have a sharp tapered shape to minimize the rupture of the tissue upon insertion.

### Design of the brain slice perfusion system

The microneedles were designed to have a thin body with a tapered sharp tip and a microfluidic port along the side of the tower to deliver medium to the interior of the tissue. Intuitively, thin sharp tips are expected to minimize trauma to the tissue. Several different examples of sharp microneedles have been previously reported in the literature (Chandrasekaran et al., 2003; McAllister et al., 2000). The SU-8 device described here has a tower height and substrate thickness that spans approximately one millimeter. When SU-8 of this thickness is processed using standard photolithography, the sidewalls tend to have a tapered shape due to the effects of UV light diffraction. The tapered tower shape facilitates further sharpening by reactive ion etching (RIE). Although some silicon microneedles have been created using similar techniques, the processing time for etching silicon needles is approximately 30 times longer than the five to ten minute etching time for SU-8 needles (Paik et al., 2004; Wilke et al., 2005). Figure 1 shows the SU-8 microneedle arrays that were sharpened from tapered tower arrays by RIE processing.

Microfluidic channels for medium delivery were created via excimer laser processing (Jolic et al., 2004). The fluidic ports were placed on the tower sidewalls for fluid delivery to the interior region of the slice. Figure 2 shows the hollow SU-8 microneedle arrays machined with different channel sizes. The location of the side-opening ports and the size of the holes may be adjusted by varying the laser's parameters. Machining the channels off-center retains the tip sharpness and creates a port with an oblong opening; while the oval shape is inherent to the microneedle fabrication method, it may also enable better perfusion of cell growth media due to the larger projected area of the channel opening.

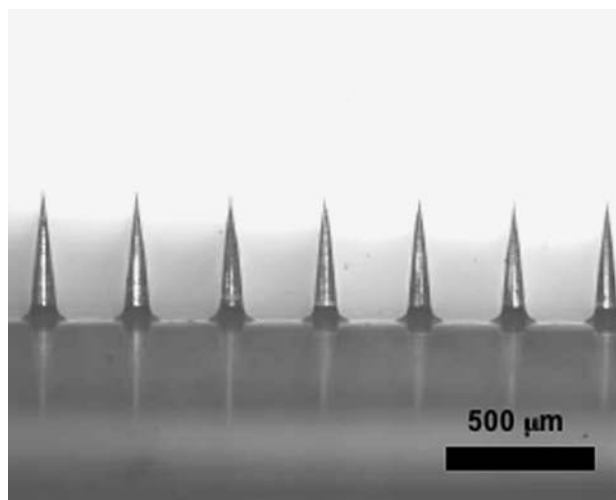


**Fig. 1** Photomicrograph of SU-8 microneedle arrays. The microneedles have been sharpened from tapered tower arrays by RIE processing

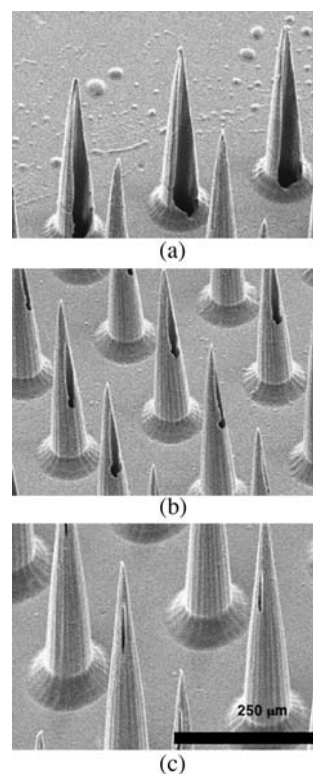


**Fig. 2** Scanning electron micrograph of SU-8 hollow microneedle arrays with fluidic channels machined at different diameters: (a) 50  $\mu\text{m}$  (b) 20  $\mu\text{m}$  (c) 10  $\mu\text{m}$ . The channel is placed off-center for all arrays to preserve the pointed tip of the needle and maximize the open area of the port. The arrays used in biological testing had channels 20  $\mu\text{m}$  in diameter

### Materials and methods

#### Fabrication sequence

The microfluidic needles are fabricated by a three-process sequence: (1) photolithographic definition of the SU-8 towers;

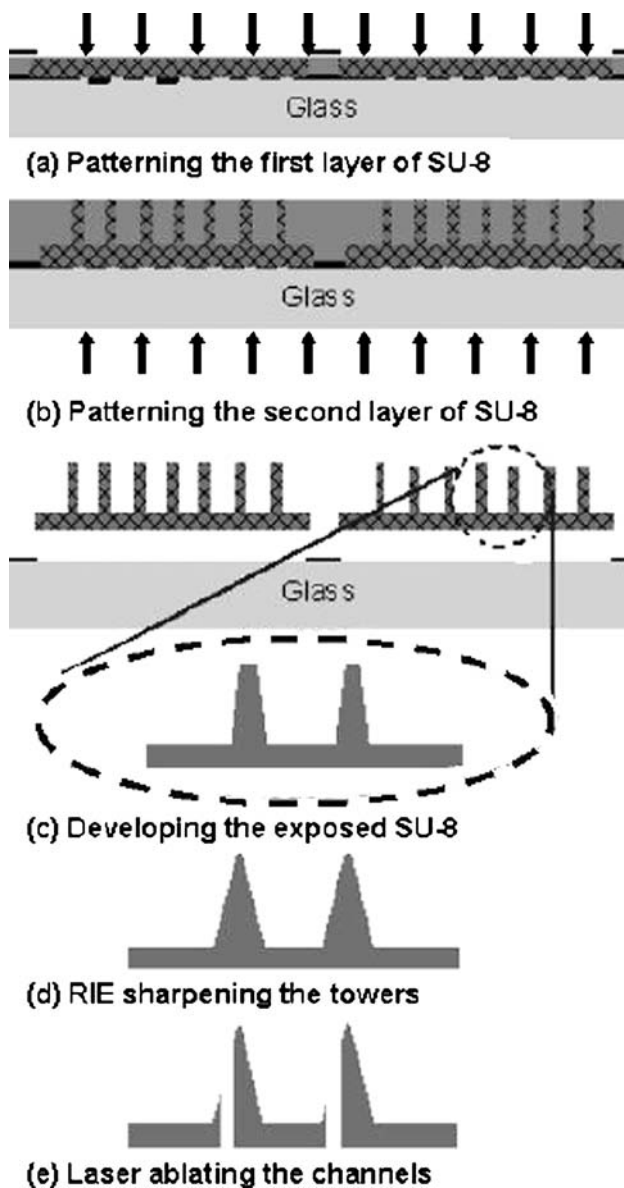


**Fig. 3** The three-process fabrication sequence is outlined in the schematic above. The photolithography is shown in steps (a–c), where two layers of SU-8 are patterned and then simultaneously developed. Then the towers are sharpened by RIE processing. Last, the channels are created via excimer laser ablation

(2) reactive ion etching for sharpened tips; (3) microchannel definition via laser ablation (Fig. 3). A chromium patterned glass plate was used as the substrate to process the SU-8 and as the backside exposure photolithography mask for the towers (Choi et al., 2005; Yoon et al., 2006). One hundred  $\mu\text{m}$  thick SU8 2025 (Microchem Corp.; Newton, MA) was spin-coated on the chromium-patterned side of the glass. After soft baking (2 h at  $95^\circ\text{C}$  on a hotplate), the sample was exposed ( $800\text{ mJ}/\text{cm}^2$ ) to make SU-8 substrates for the towers. Without further processing, the second layer of SU-8 was added for a total thickness of approximately  $600\ \mu\text{m}$ .

Backside exposure ( $5000\text{ mJ}/\text{cm}^2$ ) of the sample was performed to define the towers after soft baking (20 h at  $95^\circ\text{C}$  on a hotplate). The sample was post-exposure baked (2 h at  $95^\circ\text{C}$  on a hotplate), and developed with PGMEA (Microchem Corp.) to define both the first and second layers of SU-8. Using the patterned chromium substrates and the backside exposure, the  $600\ \mu\text{m}$  thick tapered towers were generated on the SU-8 substrate.

The sharp microneedle tips were made using an isotropic reactive ion etch (700 Series Wafer/Batch Plasma Processing System, Plasma-Therm Inc.; St. Petersburg, FL) under the following conditions: gas ratio:  $\text{CHF}_3(10\text{ sccm})/\text{O}_2(100\text{ sccm})$ , pressure: 1000 mTorr, and power: 100 W, etch rate:  $2\ \mu\text{m}/\text{min}$ . The high pressure was selected to maximize both the degree of etch isotropy and the lateral etch rate. The power level was kept low enough to control the etching speed and maintain surface smoothness. Figure 4 shows the progress of RIE processing at two-minute intervals. Figure 4(a) shows the tapered towers just after the photolithography processes. Figures 4(b)–(f) show the process of sharpening the SU-8 needles by increasing the RIE process time. Because the RIE etch processes were checked every minute, the practical etch rate was different from the non-continuous etch tests, due to the gas stabilization time in the RIE chamber at the beginning of the process. The needle structures in Fig. 4(h) were etched for five minutes without interruption, producing a shape that was almost identical to the nine minute etch in Fig. 4(f) that was stopped for measurement at one-minute intervals. The needle height can be controlled with relative ease by varying the etching time. As shown in Figs. 4(b)–(f), the height of the needles varies inversely with tip sharpness. Further etching after creating sharp tips generated residues on the tips as shown in Fig. 4(f), yet the residues could be easily removed by 10 s of sonication as shown in Fig. 4(g). Although the height of the needles can be controlled by the thickness of the spin-coated SU-8, the RIE process provides flexibility in the structure design by utilizing the etch time to vary the needle height and sharpness.

After making the sharp SU-8 needles, the next step was laser ablating the holes through the microneedles and substrate, with the channels located off-center but parallel to the tower axis. This created perfusion channels that terminate in ports midway along the needle shaft. The anisotropy and high ablation rate of the excimer laser on SU-8 make it possible to generate  $600\text{-}\mu\text{m}$  length,  $20\text{-}\mu\text{m}$  diameter channels inside the SU-8 needles. Laser ablation was done in two steps. First a  $100\ \mu\text{m}$  diameter laser beam was used to machine large channel holes from the back of the substrate that terminated at just below the top of the substrate (Fig. 5). Subsequently, a  $20\ \mu\text{m}$  laser beam was used to create the fluidic channel through the height of the needle. The two channels are visible in the scanning electron micrographs shown in Fig. 6. The  $20\ \mu\text{m}$  channel is visible in Fig. 6(b). This two-step laser

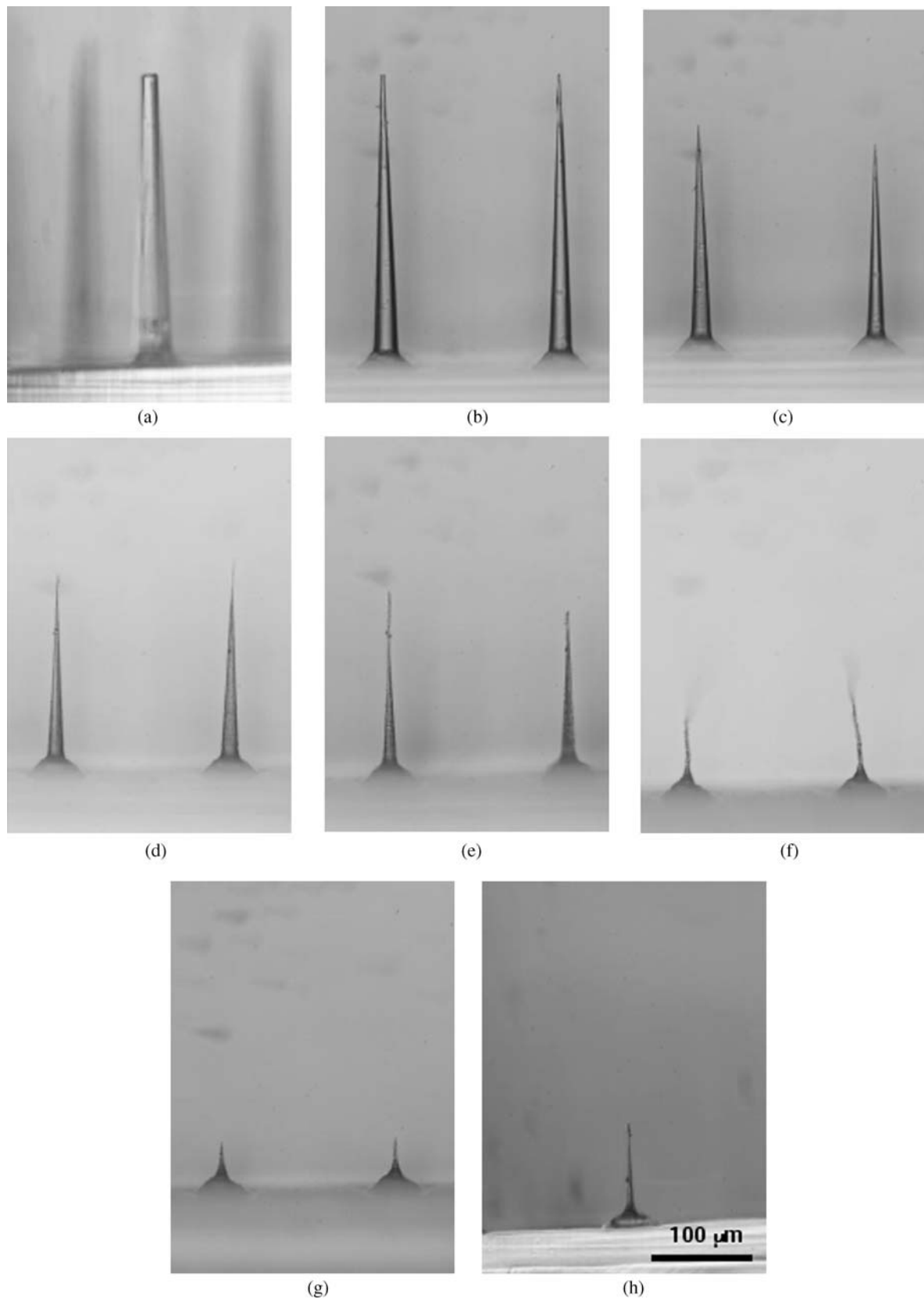


**Fig. 4** Photomicrographs show the effect of RIE processing on microneedles. The images were taken at two-minute intervals. The needles are progressively sharpened (a–d) until the process degrades the structure (e–h)

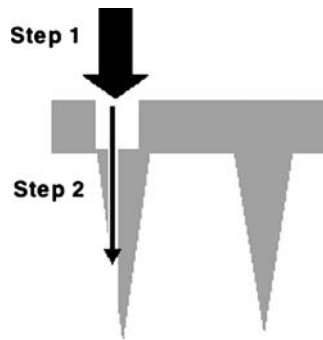
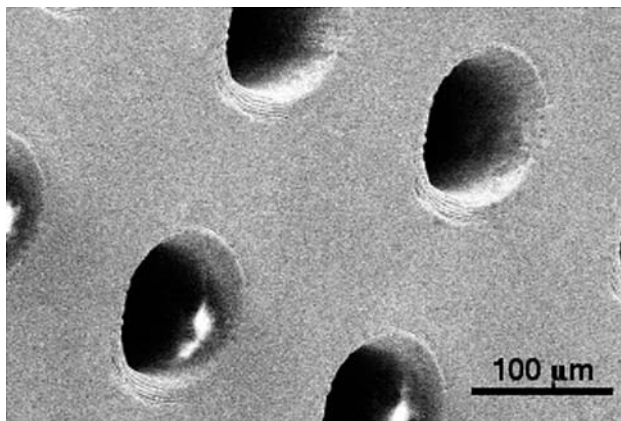
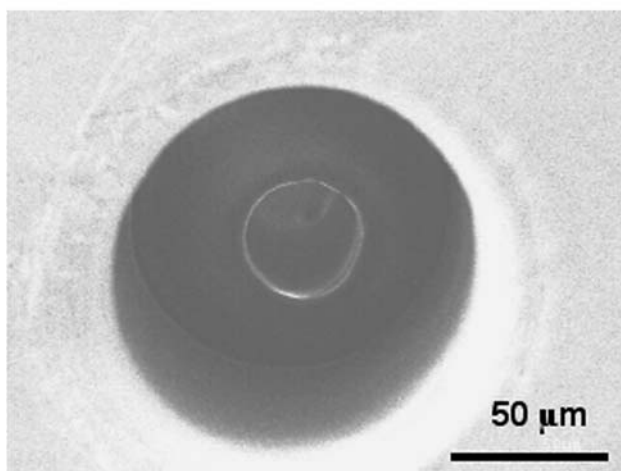


**Fig. 5** The laser ablation is a two-step process. Initially, a  $100\ \mu\text{m}$  hole is created at the back of the substrate. A  $20\ \mu\text{m}$  hole is then continued through the length of the microneedle. The size of the hole is determined by the diameter of the excimer laser



(a)

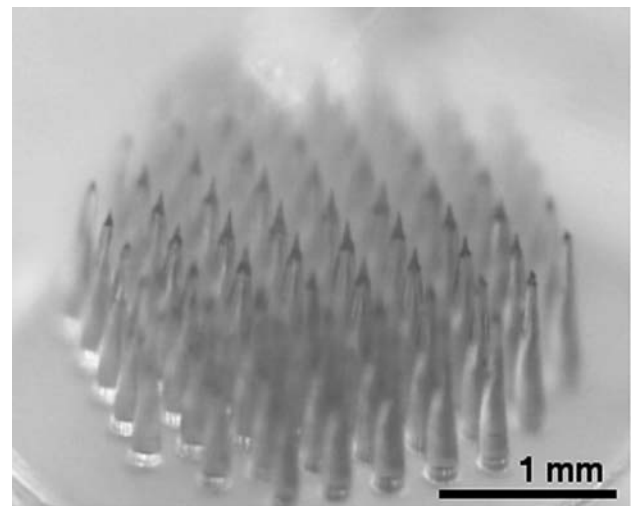


(b)

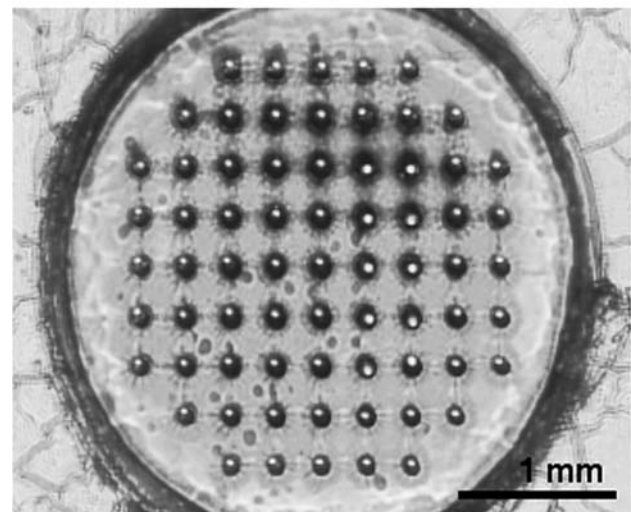
**Fig. 6** SEM micrographs show (a) the interior surface, and (b) the opening of the smaller channel after laser ablation

ablation process was used to minimize both fluidic resistance and machining time.

Using this process, perfusion tower arrays on  $2.7\ \text{mm}$  diameter circular disks were generated for brain slice culture systems. Figure 7(a) shows the microneedle arrays on circular SU-8 substrates. Figure 7(b) shows the fluidic channels



(a)



(b)

**Fig. 7** Photomicrographs of the completed microneedle arrays are shown from (a) a top view and (b) a bottom view, from which the channel openings are visible

inside the microneedles. The structure was illuminated from the backside to provide a clear view of the laser ablated fluidic channels. The microneedle array was able to pierce a  $500\ \mu\text{m}$  thick brain slice (Fig. 8a), demonstrating that the degree of sharpness was sufficient.

#### Integration of fluidic systems

For the integration of microneedle structures to the fluidic system, the needle array was connected to a polymethyl methacrylate (PMMA) manifold, with a large reservoir relative to the channel diameter to allow for equalized pressure-driven flow at each needle. A  $35\ \text{mm}$  diameter polystyrene Petri dish was also attached to ensure that the brain slice was bathed in media. Figure 8(a) shows the

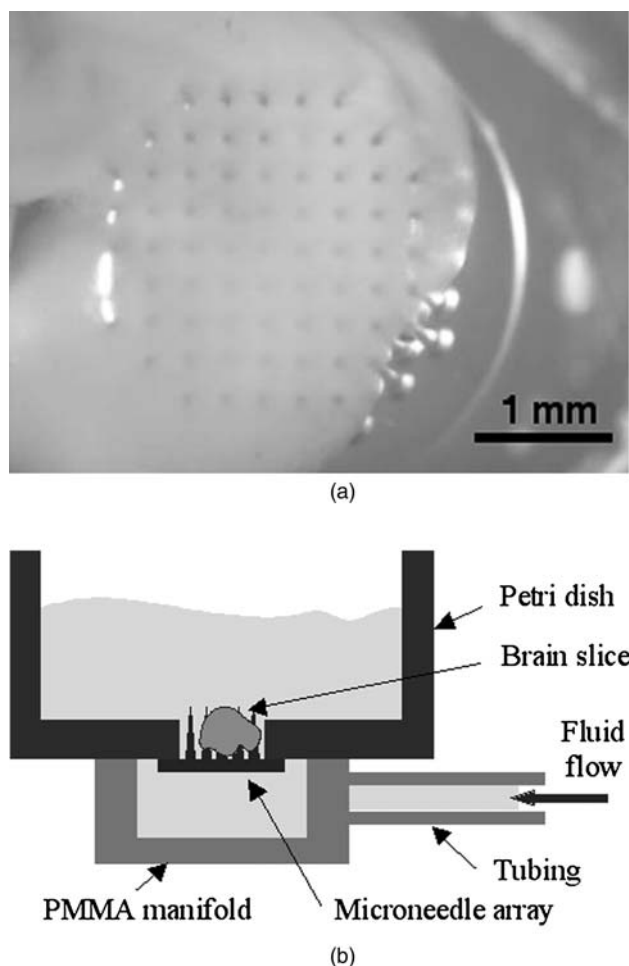


**Fig. 8** (a) A photomicrograph shows the microneedle array perfusing a brain slice. The microfluidic perfusion system integrates microneedle arrays in a packaged system for fluid containment

assembled microneedle array while perfusing a slice and Fig. 8(b) shows a conceptual side view of the system. Nanochem fittings and small-bore teflon tubing (Upchurch; Oak Harbor, WA) were used to connect to a 3 ml polypropylene syringe (BD; Franklin Lakes, NJ). The flow rate was established via syringe pump (KD scientific; Holliston, MA). For sterile preparation, while under a UV light in a biosafety cabinet, the system was flushed via syringe pump (flow rate 1 ml/hr) for 30 min each with sterile filtered ethanol, sterile filtered water, 1 mg/ml of poly-L-lysine (Sigma; St Luis, MO) in sterile filtered water, and then cell-growth media.

### Brain slice methods

Hippocampal brain tissue was isolated from postnatal Sprague Dawley rat pups at day nine (Gahwiler et al., 1997). Pups were anesthetized with 5% isofurane in oxygen prior to decapitation and harvest, which was performed within ten minutes of sacrifice on chilled surfaces to maximize

tissue viability. The hippocampi were removed from the brain and sectioned into 400  $\mu\text{m}$  thick slices using a McIlwain Tissue Chopper (Mickly Laboratories and Engineering; Surrey, England). The slices were separated in Gey's balanced salt solution (Sigma; St Luis, MO) and placed on an array. Culture medium was composed of 25% horse serum, 50% OptiMEM, 25% Hank's buffered salt solution, supplemented with 25 mM D-glucose and 1 mM L-glutamine (Invitrogen; Carlsbad, CA.). Tissue was kept in a humidified incubator with 5%  $\text{CO}_2$  at 36°C. Media was delivered to the tissue at a flow rate of 0.4  $\mu\text{l/h}$  per capillary, translating to a total flow rate of 40  $\mu\text{l/h}$ . Prior to imaging, the samples were fluorescently stained with Hoechst 33258 (1.6  $\mu\text{M}$ ) and propidium iodide (PI, 3  $\mu\text{M}$ , Molecular Probes; Eugene, OR), to identify cell nuclei and to label dead cells, respectively. The probes were incubated at 36°C on the tissue for 30 min without disruption of perfusion. Tissue was imaged using confocal microscopy (Multi Photon Excitation Confocal Microscope: LSM 510 NLO META, Carl Zeiss Inc; Oberkochen, Germany), with images taken at 10  $\mu\text{m}$  intervals through the height of the tissue. The Institutional Animal Care and Use Committee at the Georgia Institute of Technology approved all procedures involving animals.

### Results

The images shown in Fig. 8 show the viability of the tissue approximately 150  $\mu\text{m}$  from the bottom of the device after four hours of perfusion at 36°C. Because some settling occurs after slicing, 150  $\mu\text{m}$  is approximately the middle of the slice thickness as assessed from the confocal scan through the thickness of the tissue (data not shown). The viability is clearly differentiated between the slices with and without perfusion by prominent PI staining of dead cell nuclei in the non-perfused slice. The dark circular regions in the non-perfused sample are the regions occupied by the microneedles. The tissue is thoroughly stained with PI, indicating that the viability is either low or non-existent. The slice with perfusion does have some cell death, which is unavoidable after dissection, but the perfused slice viability is largely intact.

### Discussion and conclusion

Brain tissue is very sensitive to disruptions in its metabolite supply as evidenced by the incidence and severity of injury in stroke victims after the blood supply to the brain is stopped for a short period of time (Radisic et al., 2006). *Ex vivo* and *in vitro* brain slices enable the study of viable tissue, but change the tissue's environmental conditions. Investigations are normally conducted at below-physiological

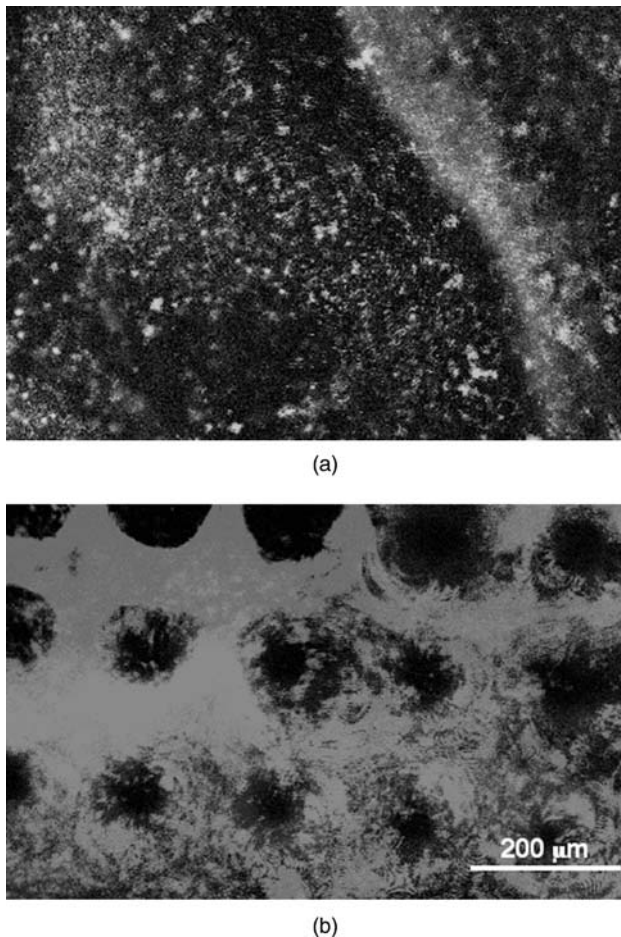


**Fig. 9** Vital staining of brain tissue from (a) perfused and (b) non-perfused samples. The microneedles are visible as the dark regions in the otherwise prominently stained tissue of the non-perfused sample

temperatures, and often at room temperature for short term studies (Heuschkel et al., 2002; Wu et al., 2005). The reduced temperature is an effective means to slow the tissue metabolism, thereby reducing the requirements for nutrient and waste exchange. Additionally, the maximum size of the tissue is always constrained, with some researchers devising innovative resection protocols to keep networks intact while exposing the maximum tissue surface area (Wu et al., 2005). In the data shown here (Fig. 9), a 400  $\mu\text{m}$  slice shows very poor viability after 4 h at 36°C. The likely cause of low viability is a rapid consumption of the available oxygen. The perfused media provides an oxygen supply along with convective nutrient and waste exchange and has proved to be a successful strategy for short-term preservation of viability. Perfusion has also been tested with hippocampal slices for 3 days on a silica capillary array and shown to improve viability over an extended time period (McClain et al., 2005). The limitation with the silica capillaries was the lack of manufacturability and the time-intensive fabrication. We have overcome this difficulty using a manufacturable SU8-based design. Perfusion by a 3D microfluidic device is intended

to circumvent some of the constraints found with *in vitro* thick tissue studies, for brain tissue and potentially other tissue types. We have demonstrated the successful fabrication of a 3D microperfusion system and validated its short-term functionality. Future studies will focus on viability with perfusion over longer time periods.

**Acknowledgments** This work was supported by the National Institutes of Health (NIH) Bioengineering Research Partnership Grant (1 R01 EB00786).

## Reference

- C.J. Bettinger, E.J. Weinberg, K.M. Kulig, J.P. Vacanti, Y.D. Wang, J.T. Borenstein, and R. Langer, *Adv. Mater.* **18**, 165 (2006).
- L.E. Buckby, R. Mummery, M.R. Crompton, P.W. Beesley, and R.M. Empson, *Dev. Brain Res.* **150**, 1 (2004).
- S. Chandrasekaran, J.D. Brazzle, and A.B. Frazier, *J. Microelectro. Sys.* **12**, 281 (2003).
- Y. Choi, S. Choi, R.H. Shafer, and M.G. Allen, In the Thirteenth International Conference on Solid-State Sensors, Actuators, and Microsystems (Transducer Research Foundation, San Diego, 2005), p. 1986.
- A. De Simoni, C.B. Griesinger, and F.A. Edwards, *J. Physiol.-London* **550**, 135 (2003).
- B.H. Gahwiler, M. Capogna, D. Debanne, R.A. McKinney, and S.M. Thompson, *Trends Neurosci.* **20**, 471 (1997).
- M.E. Gomes, H.L. Holtorf, R.L. Reis, and A.G. Mikos, *Tissue Eng.* **12**, 801 (2006a).
- M.E. Gomes, R.L. Reis, and A.G. Mikos, *Adv. Mater. Forum Iii, Pts 1 and 2* 514–516, 980 (2006b).
- M. O. Heuschkel, M. Fejtl, M. Raggenbass, D. Bertrand, and P. Renaud, *J. Neurosci. Meth.* **114**, 135 (2002).
- K.I. Jolic, M.K. Ghantasala, and E.C. Harvey, *J. Micromech. Microeng.* **14**, 388 (2004).
- B.W. Kristensen, J. Noraberg, and J. Zimmer, *Brain Res.* **973**, 303 (2003).
- D.V. McAllister, M.G. Allen, and M.R. Prausnitz, *Annu. Rev. Biomed. Eng.* **2**, 289 (2000).
- M.A. McClain, M.C. LaPlaca, and A.B. Frazier, A. In the Ninth International Conference on Miniaturized Systems for Chemistry and Life Sciences (Transducer Research Foundatin, San Diego, 2005), p. 897.
- K. Mehta and J.J. Linderman, *Biotechnol. Bioeng.* **94**, 596 (2006).
- J. Noraberg, B.W. Kristensen, and J. Zimmer, *Eur. J. Neurosci.* **12**, 238 (2000).
- S.J. Paik, A. Byun, J.M. Lim, Y. Park, A. Lee, S. Chung, J.K. Chang, K. Chun, and D.D. Cho, *Sens. Actu. A-Phys.* **114**, 276 (2004).
- M. Radisic, J. Malda, E. Epping, W.L. Geng, R. Langer, and G. Vunjak-Novakovic, *Biotechnol. Bioeng.* **93**, 332 (2006).
- G. Vunjak-Novakovic, M. Radisic, and B. Obradovic, *J. Chem. Technol. Biotechnol.* **81**, 485 (2006).
- N. Wilke, A. Mulcahy, S.R. Ye, and A. Morrissey, *Microelectr. J.* **36**, 650 (2005).
- C.P. Wu, W.P. Luk, J. Gillis, F. Skinner, and L. Zhang, *J. Neurophysiol.* **93**, 2302 (2005).
- C.P. Wu, H. Shen, W.P. Luk, and L. Zhang, *J. Physiol.-London* **540**, 509 (2002).
- X. Xu, J.P.G. Urban, U. Tirlapur, M.H. Wu, Z. Cui, and Z.F. Cui, *Biotechnol. Bioeng.* **93**, 1103 (2006).
- Y.K. Yoon, J.S. Kenney, A.T. Hunt, and M.G. Allen, *J. Micromech. Microeng.* **16**, 225 (2006).